

Subject Section

Empowering AI drug discovery with explicit and implicit knowledge

Yizhen Luo^{1,2}, Kui Huang³, Massimo Hong², Kai Yang¹, Jiahuan Zhang¹, Yushuai Wu¹ and Zaiqing Nie^{1,*}

¹Institute for AI Industry Research (AIR), Tsinghua University, Beijing, 100084, China

²Department of Computer Science and Technology, Tsinghua University, Beijing, 100084, China

³School of Software and Microelectronics, Peking University, Beijing, 100871, China

*To whom correspondence should be addressed.

Associate Editor: XXXXXXX

Received on XXXXX; revised on XXXXX; accepted on XXXXX

Abstract

Motivation: Recently, research on independently utilizing either explicit knowledge from knowledge graphs or implicit knowledge from biomedical literature for AI drug discovery has been growing rapidly. These approaches have greatly improved the prediction accuracy of AI models on multiple downstream tasks. However, integrating explicit and implicit knowledge independently hinders their understanding of molecules.

Results: We propose DeepEIK, a unified deep learning framework that incorporates both explicit and implicit knowledge for AI drug discovery. We adopt feature fusion to process the multi-modal inputs, and leverage the attention mechanism to denoise the text information. Experiments show that DeepEIK significantly outperforms state-of-the-art methods on crucial tasks in AI drug discovery including drug-target interaction prediction, drug property prediction and protein-protein interaction prediction. Further studies show that benefiting from explicit and implicit knowledge, our framework achieves a deeper understanding of molecules and shows promising potential in facilitating drug discovery applications.

Availability: The DeepEIK framework and datasets are available at <https://drive.google.com/drive/folders/1pz4QZEmcZrBU5JAJIlyMNVMrBFEXN4SN?usp=sharing>.

Contact: zaiqing@air.tsinghua.edu.cn

Supplementary information: Supplementary data are available at *Bioinformatics* online.

1 Introduction

Drug discovery aims to design molecules or compounds that respond to a certain disease and reduce their potential side effects on patients (Drews, 2000; Lomenick *et al.*, 2011; Pushpakom *et al.*, 2019). In real-world applications, human experts typically grasp molecular knowledge from multi-modal information sources including molecule structure, knowledge bases and biomedical literature to guide the research process. On the one hand, **explicit knowledge in knowledge bases** in the form of highly-reliable relationships between biomedical entities including drugs, proteins, genes and diseases plays a significant role in drug discovery. Recently, many large-scale biomedical knowledge graphs such as KEGG (Kanehisa *et al.*, 2007), BioKG (Walsh *et al.*, 2020) and PharmKG (Zheng *et al.*, 2021) have been built. On the other hand, **implicit knowledge in biomedical documents** in the form of natural language consists abundant molecular expertise (Searls, 2005). Search engines like PubChem (Kim

et al., 2016) and Uniprot (Consortium, 2015) provide summarized textual descriptions for drugs and proteins, and libraries like PubMed and bioRxiv hold billions of biomedical publications. The explosive amount of explicit and implicit knowledge calls for data-greedy deep learning models to comprehensively understand molecules and assist drug discovery.

Recently, research on independently utilizing either explicit or implicit knowledge for AI drug discovery has been growing rapidly. These approaches have greatly improved the prediction accuracy of AI models on multiple downstream tasks. For example, in drug-target interaction prediction, multiple strategies (Thafar *et al.*, 2020; Ye *et al.*, 2021; Yu *et al.*, 2022) have demonstrated the superiority of combining relational and topological information from knowledge graphs with molecule structure. In drug-drug interaction prediction, structural characteristics are assisted by relational or textual characteristics in isolation to better identify the relationships between drugs (Asada *et al.*, 2018; Zhang *et al.*, 2017; Lin *et al.*, 2020). However, existing models are mostly restricted to a single task and, to the best of our knowledge, none of them attempt to fuse both

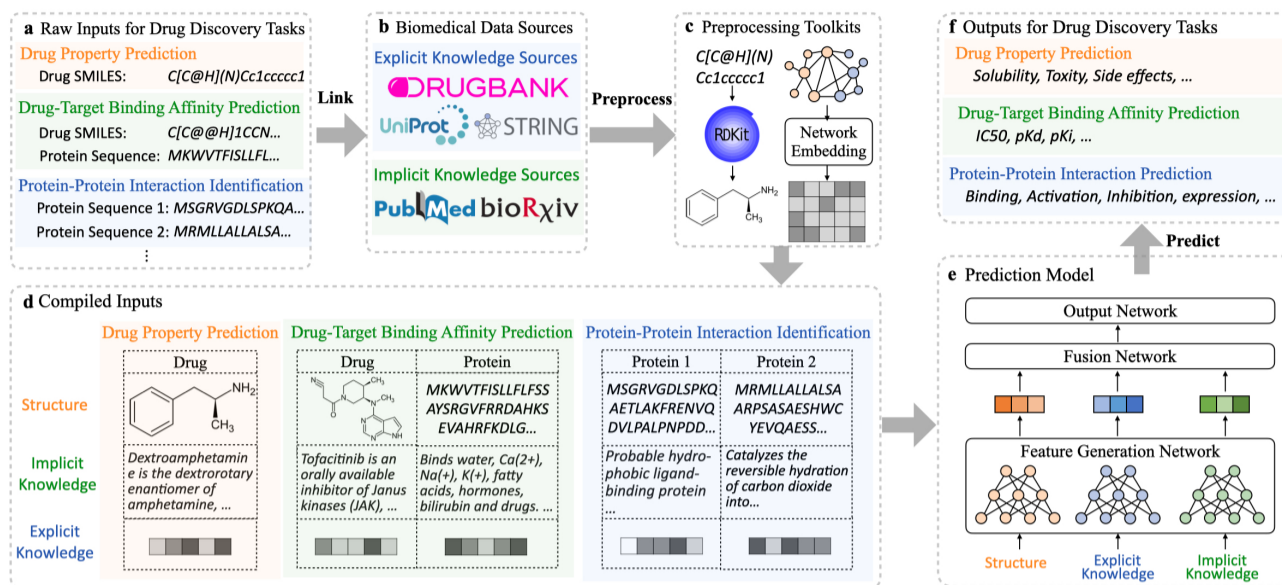


Fig. 1. The workflow of DeepEIK, a deep learning framework that integrates explicit and implicit for AI drug discovery. (a) Drug SMILES and protein sequences are linked to (b) public databases and biomedical documents to obtain interacting relationships and texts. The heterogeneous data are preprocessed by (c) computational toolkits to formulate (d) the compiled inputs, which are fed into (e) the prediction model to calculate (f) the desired outputs for downstream tasks.

explicit and implicit knowledge with structural characteristics. This limits not only the application scope but also the capability of AI systems to holistically understand the intrinsic properties and functions of molecules. Therefore, AI systems integrating both explicit and implicit knowledge for multiple AI drug discovery tasks are expected.

However, it is non-trivial to jointly exploit the advantages of explicit and implicit knowledge for the following two major challenges. First, it is hard to learn meaningful molecule representations from multiple modalities in a unified framework. Compared with the concise molecule structure of drugs and proteins, knowledge graphs and biomedical texts are of greater abundance, and their data forms are more complex (Zeng *et al.*, 2022; Ye *et al.*, 2021). Second, inevitable noises from external information sources, biomedical texts in particular, bring challenges of extracting relevant knowledge from complicated inputs (Subramaniam *et al.*, 2009). Within the lengthy descriptive paragraphs of biomedical entities, only a few sentences are strongly related to their properties and functions. To better assist downstream tasks, AI models should focus on important sentences and filter out noises.

In this work, we present DeepEIK, a unified deep learning framework that incorporates both explicit and implicit knowledge for AI drug discovery. The framework is designed to be applicable to multiple downstream tasks. We first obtain external explicit and implicit knowledge inputs from extensive public information sources. Then, we solve the multi-modal learning problem with a feature fusion technique. Specifically, we transform the heterogeneous inputs into dense feature vectors by independent encoders that enjoy both effectiveness and efficiency. Then, we design a novel fusion network that adopts the attention mechanism (Kim *et al.*, 2017) to denoise and fuse the learned heterogeneous features. Under the guidance of structural knowledge and explicit knowledge, the attention module could assign greater weights to relevant sentences, thus improving the quality of implicit knowledge features and making better predictions.

Comprehensive experiments on a series of AI drug discovery tasks demonstrate the capability of DeepEIK in uncovering the properties and relationships of molecules. DeepEIK brings considerable improvements over state-of-the-art models on several AI drug discovery tasks, boosting the performance by 2.9% on average in ROC_AUC on drug-target interaction prediction, 3.0% on average in ROC_AUC on drug property

prediction, and 11.2% on average in accuracy on protein-protein interaction prediction. Additionally, in the qualitative analysis of searching drug candidates for ACE2, 4 out of our 5 prioritized drugs are validated by recent pharmaceutical studies. In brief, the success of DeepEIK manifests the promising potential of combining structural, explicit and implicit knowledge for AI drug discovery.

Our major contributions are summarized as follows:

- (1) We present DeepEIK, a deep learning framework that combines both explicit and implicit knowledge with molecule structure to facilitate AI drug discovery.
- (2) We design a fusion network which adopts the attention mechanism to denoise textual information and integrate heterogeneous features.
- (3) We show the state-of-the-art performance of DeepEIK on numerous downstream tasks.

2 Materials and methods

In this section, we begin with the denotations and definitions of tasks DeepEIK is applied to (Section 2.1). Then, we introduce the DeepEIK framework which is illustrated in Figure 1. DeepEIK first obtains and preprocesses explicit and implicit knowledge inputs for molecules from public sources (Section 2.2). Then, it transforms the multi-modal inputs into feature vectors by independent encoders (Section 2.3). The learned representations are then denoised and fused by the fusion network (Section 2.4). Finally, the outputs for drug discovery tasks are calculated by the output network (Section 2.5).

2.1 Preliminary

DeepEIK focuses on two types of molecules, namely drugs and proteins. A drug $D \in \mathcal{D}$ is profiled as the SMILES sequence $[d_1, d_2, \dots, d_n]$. A protein $P \in \mathcal{P}$ is profiled as the amino acid sequence $[p_1, p_2, \dots, p_m]$. In this work, DeepEIK is applied to the following AI drug discovery tasks:

Drug-target interaction prediction (DTI) aims to identify the binding effects between drug compounds and protein targets. The goal is to learn a mapping function $\mathcal{F}_{DTI} : \mathcal{D} \times \mathcal{P} \rightarrow Y$. $Y = \{0, 1\}$ for binary classification and $Y = \mathbb{R}$ for regression.

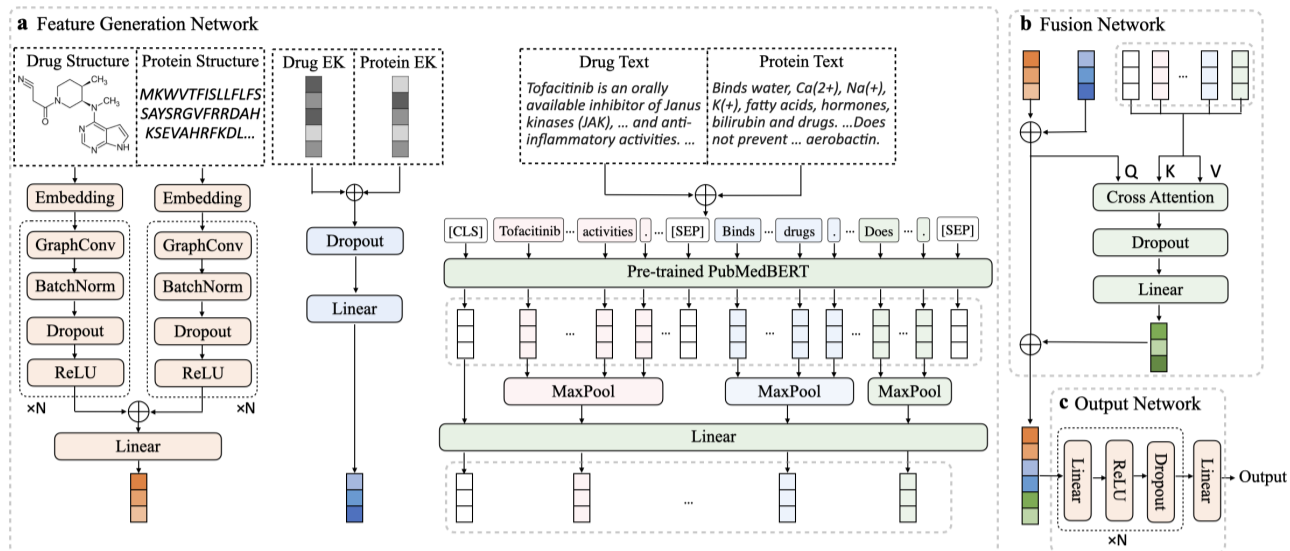


Fig. 2. The architecture of the prediction model. \oplus refers to the concatenation operation. (a) An example of the feature generation network for drug-target interaction prediction that transforms the multi-modal inputs into dense feature vectors. (b) The fusion network which denoises the textual features by the cross attention mechanism and fuses the heterogeneous features. (c) The output network that generates prediction results.

Drug property prediction (DP) aims to predict molecule properties such as toxicity and side effects. It is a binary classification task that learns a mapping function $\mathcal{F}_{DP} : \mathcal{D} \rightarrow \{0, 1\}$ to predict whether the drug D possesses the property.

Protein-protein interaction prediction (PPI) aims at predicting different types of interaction relationships between proteins. PPI is formulated as learning a mapping $\mathcal{F}_{PPI} : \mathcal{P} \times \mathcal{P} \rightarrow \{0, 1\}^T$ from a pair of proteins (P_1, P_2) to T binary values, each indicating whether there's a certain type of interaction between two proteins.

2.2 Heterogeneous inputs preparation

As shown in Figure 1(a), the majority of existing datasets for AI drug discovery only provide structural information for drugs and proteins. To apply DeepEIK on these benchmarks, the original data must be compiled with additional explicit and implicit knowledge extracted from public repositories and publications, and Figure 1(b) illustrates several representatives. To simplify the data acquisition process, we build BMKG, a dataset containing molecule structure, interacting relationships and textual descriptions for 6,917 drugs and 19,992 proteins from public sources (more details are presented in Supplementary Information). Then, given the SMILES string of a drug D or the amino acid sequence of a protein P , we compare it with molecules in BMKG to obtain its explicit knowledge (D_e for the drug and P_e for the protein) and textual description (D_i for the drug and P_i for the protein). If the exact match doesn't exist, the external knowledge inputs will be marked 'Not Available' using default values.

Additionally, we adopt preprocessing steps in Figure 1(c) to generate the desired multi-modal inputs in Figure 1(d). Specifically, we transform the SMILES string D into a 2D molecule graph $\mathcal{G} = (\mathcal{V}, \mathcal{E}, \mathcal{X})$, where \mathcal{V} is the node set, $\mathcal{E} \subset \mathcal{V} \times \mathcal{V}$ is the edge set, and $\mathcal{X} \in \mathbb{R}^{|\mathcal{V}| \times d_1}$ is the initial node feature. We also calculate an embedding matrix $H_e \in \mathbb{R}^{N \times d_2}$ to represent the explicit knowledge, where N is the number of nodes in BMKG and d_2 is the embedding dimension. Considering the scale of our dataset, we withdraw the types of nodes and links, and adopt a fast and efficient network embedding algorithm ProNE (Zhang *et al.*, 2019) to calculate network embeddings.

2.3 Multi-modal feature extraction

In this step, we employ independent single-modal encoders to transform the multi-modal inputs into dense feature vectors. The encoding architecture that learns the representations of molecule structure, explicit knowledge and implicit knowledge differs slightly for each task. The network architecture for the DTI task is illustrated in Figure 2(a).

2.3.1 Molecule structure representation

To transform the molecule structure of a drug or a protein into the feature vector $h_s \in \mathbb{R}^{d_3}$, we directly derive encoders from previous studies that capture the intrinsic nature for each task. Specifically:

For the DTI task, we follow MGraphDTA (Yang *et al.*, 2022) that proposes a multi-scale graph neural network to encode the molecule graphs \mathcal{G} and a multi-scale convolutional neural network to encode the protein sequence P . We concatenate the output of two encoders and feed it into a fully connected layer to obtain the structural representation h_s .

For the DP task, we adopt the pre-trained GIN (Xu *et al.*, 2018) in MolCLR (Wang *et al.*, 2022), a powerful neural network to encode \mathcal{G} . A fully connected layer is added to unify feature dimension and obtain h_s .

For the PPI task, we apply our method based on DeepTrio (Hu *et al.*, 2022), which employs deep CNN with a masking strategy to encode proteins. Similar to DTI, the outputs of two proteins P_1, P_2 are concatenated, and fed into a linear layer to formulate the structural representation h_s .

2.3.2 Explicit knowledge representation

For explicit knowledge, the embedding vectors for two molecules are first concatenated for DTI and PPI tasks, and then fed into a dropout layer followed by a fully connected layer to generate the explicit knowledge feature $h_e \in \mathbb{R}^{d_4}$.

2.3.3 Implicit knowledge representation

For implicit knowledge, we first concatenate the tokenized sequence of two molecules with a special token '[SEP]' for DTI and PPI tasks. In this way, the text encoder could better capture the consistent description of two molecules and understand their relationship. Next, we leverage PubMedBERT (Gu *et al.*, 2021), a language model with

12 stacked Transformer (Vaswani *et al.*, 2017) layers to transform the word sequence $W = [w_1, w_2, \dots, w_l]$ of length l into hidden features $H = [h_1, h_2, \dots, h_l] \in \mathbb{R}^{l \times d_o}$, where d_o is the output dimension of PubMedBERT. Then, we apply max-pooling over each sentence followed by a fully connected layer to obtain implicit knowledge features $h_i \in \mathbb{R}^{m \times d_5}$ for m sentences as follows:

$$\begin{aligned} s_i &= \text{MaxPool}(h_{l_i}, h_{l_i+1}, \dots, h_{r_i}) \\ h_i &= W_i[s_1, s_2, \dots, s_m] + b_i \end{aligned} \quad (1)$$

where l_i , r_i and s_i are the beginning index, ending index and feature vector of the i -th sentence, and $W_i \in \mathbb{R}^{d_o \times d_5}$, $b_i \in \mathbb{R}^{d_5}$ are model parameters. The sentence-level representations capture the semantic characteristics within each sentence, and are computationally efficient for further fusion steps.

2.4 Feature fusion

Unlike the concise features extracted from molecule structure and explicit knowledge, text information is noisy and weakly correlated. Typically, only a few sentences within the paragraph contain information relevant to the downstream task. In the fusion network illustrated in Figure 2(b), the key technique to denoise and augment implicit knowledge features is the attention mechanism (Kim *et al.*, 2017) that assigns different weights to each sentence feature. The attention module takes three inputs, namely the queries Q , the keys K and the values V . We take the concatenation result of the structural feature and explicit knowledge feature as the query vector to guide the selection process. The sentence features are regarded as the key and value vectors. The denoised implicit knowledge feature is calculated as follows:

$$\begin{aligned} Q &= h_s \oplus h_e, K = h_i, V = h_i \\ \tilde{h}_i &= \text{Attention}(Q, K, V) \\ &= \text{softmax}\left(\frac{(QW_Q)(KW_K)^T}{\sqrt{d_5}}\right)VW_V \end{aligned} \quad (2)$$

where \oplus is the concatenation operation, $W_Q \in \mathbb{R}^{(d_3+d_4) \times d_5}$, $W_K \in \mathbb{R}^{d_5 \times d_5}$, $W_V \in \mathbb{R}^{d_5 \times d_5}$ are parameter matrices, and $\tilde{h}_i \in \mathbb{R}^{d_5}$ is the denoised implicit knowledge feature. The attention module allows the fusion network to dynamically integrate information from crucial sentences and filter out noises. It also enforces the interaction between multi-modal features through back propagation.

Finally, we fuse the structural feature, explicit knowledge feature and the denoised implicit knowledge feature via concatenation, i.e. $z_0 = h_s \oplus h_e \oplus \tilde{h}_i$.

2.5 Prediction and learning objectives

As illustrated in Figure 2(c), the fused feature z_0 is fed into the output network composed of m fully connected layers with ReLU activation and dropout to generate the prediction result \tilde{y} . For classification problems, $\tilde{y} \in \mathbb{R}^C$ corresponds to the confidence score for C classes. For regression problems, $\tilde{y} \in \mathbb{R}$ is the prediction value.

DeepEIK is trained in an end-to-end manner for each task. We optimize cross entropy loss L_c for classification problems and mean squared loss L_r for regression problems. The objective functions are:

$$\begin{aligned} L_c &= - \sum_{i=1}^C y_i \log \frac{\exp(\tilde{y}_i)}{\sum_{j=1}^C \exp(\tilde{y}_j)} \\ L_r &= (y - \tilde{y})^2 \end{aligned} \quad (3)$$

where y is the ground truth.

3 Experiments and results

In this section, we first give a brief introduction of the datasets DeepEIK is tested on (Section 3.1). Then, we show the state-of-the-art performance of DeepEIK for each task (Section 3.2). We also carry out ablation studies to further investigate the impacts of explicit and implicit knowledge (Section 3.3). Finally, we show the potential of our framework in assisting real-world drug discovery applications with a case study (Section 3.4).

3.1 Datasets

We test DeepEIK on 10 benchmark datasets summarized in Table 1 (more details are presented in Supplementary Information).

Table 1. A brief summary of benchmark datasets. We present the number of drugs and proteins in the dataset (right to /) and those successfully linked to BMKG (left to /), the number of data samples, and the number of prediction objectives.

Task	Dataset	# Drugs	# Proteins	# Samples	# Tasks
DTI	Yamanishi08's	488 / 791	944 / 989	10254	1
	BMKG-DTI	2803 / 2803	2810 / 2810	47391	1
	Davis	39 / 68	337 / 379	30056	1
	KIBA	85 / 2221	221 / 279	118254	1
DP	BBBP	841 / 2039	-	2039	1
	ClinTox	556 / 1478	-	1478	2
	Tox21	2191 / 7831	-	7831	12
	SIDER	677 / 1427	-	1427	27
PPI	SHS27k	-	1632 / 1690	10928	1
	SHS148k	-	4943 / 5189	63065	1

For DTI, we adopt binary classification datasets *Yamanishi08's* (Yamanishi *et al.*, 2008) and *BMKG-DTI*. We also adopt regression datasets *Davis* (Davis *et al.*, 2011) and *KIBA* (Tang *et al.*, 2014).

For DP, we select 4 representative themes from MoleculeNet (Wu *et al.*, 2018), a widely-adopted benchmark for molecular machine learning. The binary classification datasets are *BBBP*, *ClinTox*, *Tox21*, *SIDER*.

For PPI, we revise the *SHS27k* and *SHS148k* dataset proposed by Chen *et al.* (2019). We remove duplicate samples to avoid data leakage and combine different types of labels for the same protein-protein pair to build the multi-label classification datasets.

3.2 Performance evaluation for AI drug discovery tasks

For **drug-target interaction prediction**, we choose random forest (RF) (Ho, 1995), support vector machine (SVM) (Cortes and Vapnik, 1995), DeepDTA (Öztürk *et al.*, 2018), DeepDTAF (Wang *et al.*, 2021), MGraphDTA (Yang *et al.*, 2022) and KGE_NFM (Ye *et al.*, 2021) for comparison. Experiments are conducted under 5-fold cross validation. ROC_AUC and PR_AUC under warm-start and cold-start settings are presented for Yamanishi08's and BMKG-DTI in Figure 3 and Supplementary Table 3~4. Mean square error (MSE), concordance index (CI) and r_m^2 index are presented for Davis and KIBA in Supplementary Table 5. From the results we find that under warm-start setting, DeepEIK outperforms existing methods by a wide margin. For example, on Yamanishi08's and BMKG-DTI, the absolute performance gain in terms of ROC_AUC over the state-of-the-art method MGraphDTA are 2.5% and 3.2% respectively. On Davis, DeepEIK outperforms MGraphDTA by 0.012 in MSE, 0.006 in CI and 0.043 in r_m^2 index. On KIBA, the results show little statistical difference with MGraphDTA, which could be attributed to the lack of external knowledge of drugs.

Besides, it is worth highlighting that DeepEIK consistently manifests superiority over other baselines under cold-start settings. Overall, the performance of AI models declines when drugs and proteins in the test set are unseen during training. Remarkably, on BMKG-DTI, compared

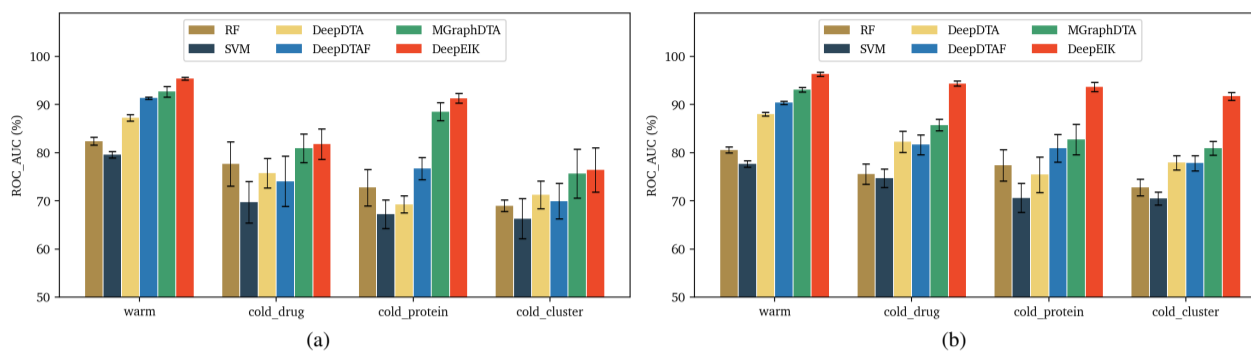


Fig. 3. Experiment results for drug-target interaction prediction. (a) ROC_AUC (%) on Yamanishi08's dataset. (b) ROC_AUC (%) on BMKG-DTI dataset.

to the warm-start results (ROC_AUC=0.963), DeepEIK could achieve competitive performance under cold-start scenarios (ROC_AUC=0.943, 0.937, 0.917 under cold-drug, cold-protein and cold-cluster setting), and the performance gain over the state-of-the-art is more profound, ranging from 8.5% to 10.9%. These results imply that DeepEIK is not memorizing superficial patterns of the input data, but learning transferable meta-knowledge from heterogeneous information sources.

Table 2. Experiment results for drug property prediction. Mean and standard deviation of test ROC_AUC (%) are reported. * These results are taken from MolCLR.

Model	BBBP	ClinTox	Tox21	SIDER	Average
RF*	71.4±0.0	71.3±5.6	76.9±1.5	68.4±0.9	72.0±2.0
SVM*	72.9±0.0	66.9±9.2	81.8±1.0	68.2±1.3	72.5±2.9
GCN*	71.8±0.9	62.5±2.8	70.9±2.6	53.6±3.2	64.7±2.4
GIN*	65.8±4.5	58.0±4.4	74.0±0.8	57.3±1.6	63.8±2.8
MolCLR*	73.6±0.5	93.2±1.7	79.8±0.7	68.0±1.1	78.7±1.0
DeepEK	75.9±1.3	93.8±1.3	81.4±1.2	71.7±0.7	80.7±1.1
DeepIK	74.6±2.3	93.4±1.2	80.1±1.3	70.6±0.6	79.7±1.6
DeepEIK ^{-attn}	77.0±1.7	93.9±2.1	81.9±1.5	72.4±0.5	81.3±1.5
DeepEIK	77.8±1.3	94.0±2.4	82.1±1.8	72.7±0.6	81.7±1.5

For drug property prediction, we compare DeepEIK with RF, SVM, GCN (Kipf and Welling, 2018), GIN (Xu *et al.*, 2018) and MolCLR (Wang *et al.*, 2022). Following Wang *et al.* (2022), we apply Scaffold split (Bemis and Murcko, 1996) on MoleculeNet datasets and report test ROC_AUC of 3 runs with different random seeds in Table 2. We observe that the structure-based model MolCLR is inferior to feature-based models on Tox21 and SIDER mainly due to insufficient training data. In comparison, DeepEIK consistently achieves the best results on these datasets. Remarkably, it yields an average of 3.0% improvement over the original MolCLR by integrating explicit and implicit knowledge.

For protein-protein interaction prediction, we implement baselines including RF, SVM, PIPR (Chen *et al.*, 2019) and DeepTrio (Hu *et al.*, 2022). We conduct 10-fold cross validation, and accuracy as well as Micro F1 score on test sets are shown in Table 3. From the results we can see that DeepEIK prominently boosts the performance of DeepTrio by 12.0% and 10.3% in terms of accuracy, and 6.5% and 5.7% in terms of Micro F1 on SHS27k and SHS148k.

The promising results of DeepEIK indicate that knowledge graphs and text descriptions contain abundant biochemical knowledge of molecules. Benefiting from these knowledge, DeepEIK could achieve a deep and comprehensive understanding of molecules and make accurate predictions on a wide range of AI drug discovery tasks.

Table 3. Experiment results for protein-protein prediction. Mean and standard deviation of test Accuracy (%) and Micro F1 (%) under 10-fold cross validation are reported.

Model	SHS27k		SHS148k	
	Acc (%)	Micro F1 (%)	Acc (%)	Micro F1 (%)
RF	63.1±0.7	80.4±0.7	70.4±0.3	84.3±0.3
SVM	59.5±1.1	80.7±0.8	59.2±0.3	80.2±0.3
PIPR	64.1±1.1	82.0±0.8	71.0±0.7	85.0±0.4
DeepTrio	66.4±1.3	83.8±0.8	72.0±0.7	86.3±0.4
DeepEK	76.8±1.2	88.9±0.8	81.0±0.8	91.1±0.5
DeepIK	70.6±1.1	86.0±0.8	73.5±0.6	87.3±0.4
DeepEIK ^{-attn}	77.5±1.0	89.7±0.7	81.8±0.5	91.6±0.2
DeepEIK	78.4±1.1	90.3±0.7	82.3±0.5	92.0±0.2

3.3 Ablation studies

Experiment results of DeepEK and DeepIK demonstrate that integrating either explicit or implicit knowledge leads to better performance, and combining both of them yields the best results. However, it is worth noting that their impacts vary on different tasks. For DTI prediction, DeepEK and DeepIK achieve similar results (0.943 v.s. 0.944 on Yamanishi 08's, and 0.954 v.s. 0.945 on BMKG-DTI in terms of ROC_AUC under warm-start setting), indicating that explicit and implicit knowledge contribute equally to this task. For DP prediction, explicit knowledge plays a more important role, bringing an average of 2.0% performance gain compared with 1.0% of implicit knowledge. Similar observations are found for PPI prediction, where DeepEK achieves order-of-magnitude advances while DeepIK only yields limited improvements (10.4% v.s. 4.2% on SHS27k and 9.0% v.s. 1.5% on SHS148k in accuracy). Overall, the performance of DeepEK is not as promising as DeepEK for the following two reasons:

(1) The scale of explicit and implicit knowledge inputs is disproportional. In our implementation, we obtain explicit and implicit knowledge inputs from BMKG which contains abundant relationships (~2.6M drug-drug edges and ~0.6M protein-protein edges) but relatively insufficient text descriptions (~67 words on average for each drug and ~85 words on average for each protein). Interestingly, we observe that drug receptors are frequently mentioned in the description (examples are shown in Supplementary Fig. 4), which explains DeepEK's promising results in predicting drug-target interactions.

(2) Extracting appropriate implicit knowledge from noisy texts is more challenging than learning from knowledge graphs. On the one hand, the proximity and structural similarity of nodes (Qiu *et al.*, 2020) in a knowledge graph could be captured by network embedding algorithms to facilitate prediction tasks. On the other hand, noises are ubiquitous in text data that describes the characteristics and relationships of molecules in natural language (Subramaniam *et al.*, 2009). To exploit the benefits of

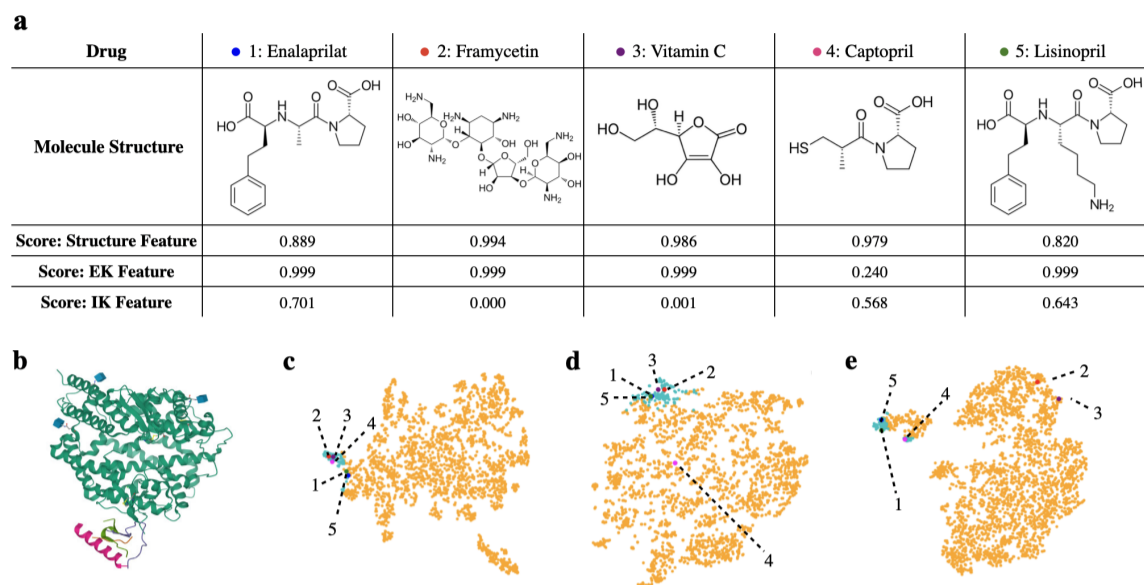


Fig. 4. A drug repurposing example for ACE2. (a) Details for each drug candidate and the prediction scores of DeepEIK when only molecule structure, explicit knowledge (EK) and implicit knowledge (IK) is considered. (b) Protein structure of ACE2. (c) Visualization of structural features. (d) Visualization of explicit knowledge features. (e) Visualization of implicit features.

implicit knowledge, AI models are required to not only understand the context but also extract relevant information from noisy inputs.

DeepEIK leverages the attention mechanism to denoise text information. To demonstrate its effectiveness, we implement DeepEIK^{-attn} that replaces the attention module with a mean-pooling layer to calculate the implicit knowledge feature \tilde{h}_i . While DeepEIK^{-attn} still outperforms DeepEK, its performance drops 0.4% on average compared with DeepEIK. Using the cross attention mechanism, we guide the process of extracting important sentences with the help of structural knowledge and explicit knowledge. In this way, DeepEIK could further improve the quality of implicit knowledge and achieve better predictive performance.

3.4 A case study in real-world drug discovery scenarios

To test the power of DeepEIK in real-world drug discovery scenarios, we conduct a case study on searching for drugs that bind with angiotensin-converting enzyme 2 (ACE2), a protein that has been proven to be an entry receptor of SARS-CoV-2 (Cuervo and Grandvaux, 2020; Li et al., 2020). We remove data samples containing ACE2 from the BMKG-DTI dataset and train DeepEIK on it. Then, we predict the probability for each drug in BMKG-DTI to bind with ACE2 and select top-5 candidates. To explore the impact of each modality, we calculate output scores when only molecule structure, explicit knowledge or implicit knowledge is considered, which are shown in Figure 4(a). We also visualize the structural feature, explicit knowledge feature and implicit knowledge feature for each drug via t-sne (Van der Maaten and Hinton, 2008) in Figure 4(c)~(e).

Among the 5 drugs DeepEIK identified, Captopril and Lisinopril are validated active compounds, and their binding affinity values tested by wet lab experiments are reported on PubChem. For the other three drugs, in vitro evidence are not available in the database. However, recent studies from biomedical domain point out that Vitamin C and Enalaprilat may have a lowering effect on the protein (Ivanov et al., 2021; Zuo et al., 2022; Moraes et al., 2021), and an in silico work suggests that Framycetin could be a potential ACE2 inhibitor (Rampogu and Lee, 2021).

While the structure-based prediction scores are relatively high for all the prioritized drugs, supporting evidence could be found from explicit and implicit knowledge. As shown in Figure 4, the prediction scores of Enalaprilat, Framycetin, Vitamin C and Lisinopril using explicit knowledge are close to 1.0, and their explicit knowledge features are

mapped closely to each other. Interestingly, over 99% of the neighboring nodes of Enalaprilat and Lisinopril are the same, and their explicit knowledge features are almost identical. As for implicit knowledge, we observe in Supplementary Figure 4 that the inhibitory effects of Enalaprilat, Captopril and Lisinopril on ACE (a homologous protein of ACE2) are pointed out in their text descriptions, and DeepEIK assigns high attention scores to the corresponding sentence. Consequently, DeepEIK is able to make confident predictions for these drugs solely based on the implicit knowledge, and the implicit knowledge features distilled by the attention module show clear clustering trends in Figure 4(e). For Vitamin C and Framycetin, however, their text information are irrelevant, and their text-based prediction scores are close to 0.

The results above show that DeepEIK is capable of searching potential drugs for "new targets" by comprehensively integrating explicit and implicit knowledge. Therefore, there is possibility for the framework to assist real-world drug discovery applications.

4 Conclusion and future work

In this article, we show the superiority of integrating both explicit and implicit knowledge for AI drug discovery. We present a unified framework DeepEIK that learns molecular knowledge from molecule structures, knowledge graphs and biomedical documents. The framework leverages feature fusion to process the multi-modal inputs, and proposes a fusion network with an attention module to denoise and integrate heterogeneous features. The effectiveness of our framework is validated by its outstanding performance on various tasks including drug-target interaction prediction, drug property prediction and protein-protein interaction prediction. DeepEIK could grasp expertise for new molecules as long as they are profiled in knowledge bases and biomedical publications. Besides, we give a brief investigation on the impacts of explicit and implicit knowledge, and highlight the attention module which alleviates the noisy text problem. Qualitative studies reveal DeepEIK's potential in assisting real-world drug discovery applications. Above all, DeepEIK makes a pioneering contribution to bridging the gap between AI drug discovery systems and human experts by integrating both explicit and implicit knowledge, which is a promising but rarely tapped research direction.

Still, several new problems arise when carrying out this work. First, the power of DeepEIK is restricted by the scale and diversity of BMKG. More drugs and proteins in pharmaceutical research field could be added to the dataset, and their descriptive texts could be enriched by combining more biomedical publications and patents. Besides, other types of entities such as diseases, genes and side-effects and their relationships could also be considered. Second, interpretable tools that reveal the interactions between substructures of molecules and background knowledge are expected. Delving deeper into substructures, DeepEIK could better understand the biochemical properties and functions of newly discovered biomedical entities whose explicit and implicit knowledge are vacant or insufficient.

Acknowledgements

We thank Beijing Academy of Artificial Intelligence (BAAI) for their supports.

References

- Asada, M. *et al.* (2018). Enhancing drug-drug interaction extraction from texts by molecular structure information. In *Proceedings of the 56th Annual Meeting of the Association for Computational Linguistics (Volume 2: Short Papers)*, pages 680–685.
- Bemis, G. W. and Murcko, M. A. (1996). The properties of known drugs. 1. molecular frameworks. *Journal of medicinal chemistry*, **39**(15), 2887–2893.
- Chen, M. *et al.* (2019). Multifaceted protein–protein interaction prediction based on siamese residual RCNN. *Bioinformatics*, **35**(14), i305–i314.
- Consortium, U. (2015). UniProt: a hub for protein information. *Nucleic acids research*, **43**(D1), D204–D212.
- Cortes, C. and Vapnik, V. (1995). Support-vector networks. *Machine learning*, **20**(3), 273–297.
- Cuervo, N. Z. and Grandvaux, N. (2020). ACE2: Evidence of role as entry receptor for sars-cov-2 and implications in comorbidities. *Elife*, **9**, e61390.
- Davis, M. I. *et al.* (2011). Comprehensive analysis of kinase inhibitor selectivity. *Nature biotechnology*, **29**(11), 1046–1051.
- Drews, J. (2000). Drug discovery: a historical perspective. *science*, **287**(5460), 1960–1964.
- Gu, Y. *et al.* (2021). Domain-specific language model pretraining for biomedical natural language processing. *ACM Transactions on Computing for Healthcare (HEALTH)*, **3**(1), 1–23.
- Ho, T. K. (1995). Random decision forests. In *Proceedings of 3rd international conference on document analysis and recognition*, volume 1, pages 278–282. IEEE.
- Hu, X. *et al.* (2022). DeepTrio: a ternary prediction system for protein–protein interaction using mask multiple parallel convolutional neural networks. *Bioinformatics*, **38**(3), 694–702.
- Ivanov, V. *et al.* (2021). Inhibition of ACE2 expression by ascorbic acid alone and its combinations with other natural compounds. *Infectious Diseases: Research and Treatment*, **14**, 1178633721994605.
- Kanehisa, M. *et al.* (2007). KEGG for linking genomes to life and the environment. *Nucleic acids research*, **36**(suppl_1), D480–D484.
- Kim, S. *et al.* (2016). PubChem substance and compound databases. *Nucleic acids research*, **44**(D1), D1202–D1213.
- Kim, Y. *et al.* (2017). Structured attention networks. In *International Conference on Learning Representations*.
- Kipf, T. N. and Welling, M. (2018). Semi-supervised classification with graph convolutional networks. In *International Conference on Learning Representations*.
- Li, Y. *et al.* (2020). Physiological and pathological regulation of ACE2, the SARS-CoV-2 receptor. *Pharmacological research*, **157**, 104833.
- Lin, X. *et al.* (2020). KGNN: Knowledge graph neural network for drug–drug interaction prediction. In *IJCAI*, volume 380, pages 2739–2745.
- Lomenick, B. *et al.* (2011). Identification of direct protein targets of small molecules. *ACS chemical biology*, **6**(1), 34–46.
- Moraes, D. S. *et al.* (2021). Enalapril improves obesity associated liver injury ameliorating systemic metabolic markers by modulating angiotensin converting enzymes ACE/ACE2 expression in high-fat feed mice. *Prostaglandins & Other Lipid Mediators*, **152**, 106501.
- Öztürk, H. *et al.* (2018). DeepDTA: deep drug–target binding affinity prediction. *Bioinformatics*, **34**(17), i821–i829.
- Pushpakom, S. *et al.* (2019). Drug repurposing: progress, challenges and recommendations. *Nature reviews Drug discovery*, **18**(1), 41–58.
- Qiu, J. *et al.* (2020). Gcc: Graph contrastive coding for graph neural network pre-training. In *Proceedings of the 26th ACM SIGKDD International Conference on Knowledge Discovery & Data Mining*, pages 1150–1160.
- Rampogu, S. and Lee, K. W. (2021). Pharmacophore modelling-based drug repurposing approaches for SARS-CoV-2 therapeutics. *Frontiers in Chemistry*, **9**, 636362.
- Searls, D. B. (2005). Data integration: challenges for drug discovery. *Nature reviews Drug discovery*, **4**(1), 45–58.
- Subramaniam, L. V. *et al.* (2009). A survey of types of text noise and techniques to handle noisy text. In *Proceedings of The Third Workshop on Analytics for Noisy Unstructured Text Data*, pages 115–122.
- Tang, J. *et al.* (2014). Making sense of large-scale kinase inhibitor bioactivity data sets: a comparative and integrative analysis. *Journal of Chemical Information and Modeling*, **54**(3), 735–743.
- Thafar, M. A. *et al.* (2020). DTiGEMS+: drug–target interaction prediction using graph embedding, graph mining, and similarity-based techniques. *Journal of Cheminformatics*, **12**(1), 1–17.
- Van der Maaten, L. and Hinton, G. (2008). Visualizing data using t-SNE. *Journal of machine learning research*, **9**(11).
- Vaswani, A. *et al.* (2017). Attention is all you need. *Advances in neural information processing systems*, **30**.
- Walsh, B. *et al.* (2020). BioKG: A knowledge graph for relational learning on biological data. In *Proceedings of the 29th ACM International Conference on Information & Knowledge Management*, pages 3173–3180.
- Wang, K. *et al.* (2021). DeepDTAF: a deep learning method to predict protein–ligand binding affinity. *Briefings in Bioinformatics*, **22**(5), bbab072.
- Wang, Y. *et al.* (2022). Molecular contrastive learning of representations via graph neural networks. *Nature Machine Intelligence*, **4**(3), 279–287.
- Wu, Z. *et al.* (2018). MoleculeNet: a benchmark for molecular machine learning. *Chemical science*, **9**(2), 513–530.
- Xu, K. *et al.* (2018). How powerful are graph neural networks? In *International Conference on Learning Representations*.
- Yamanishi, Y. *et al.* (2008). Prediction of drug–target interaction networks from the integration of chemical and genomic spaces. *Bioinformatics*, **24**(13), i232–i240.
- Yang, Z. *et al.* (2022). MGraphDTA: deep multiscale graph neural network for explainable drug–target binding affinity prediction. *Chemical science*, **13**(3), 816–833.
- Ye, Q. *et al.* (2021). A unified drug–target interaction prediction framework based on knowledge graph and recommendation system. *Nature communications*, **12**(1), 1–12.
- Yu, L. *et al.* (2022). HGDTI: predicting drug–target interaction by using information aggregation based on heterogeneous graph neural network. *BMC bioinformatics*, **23**(1), 1–18.
- Zeng, Z. *et al.* (2022). A deep-learning system bridging molecule structure and biomedical text with comprehension comparable to human professionals. *Nature communications*, **13**(1), 1–11.
- Zhang, J. *et al.* (2019). ProNE: Fast and scalable network representation learning. In *IJCAI*, volume 19, pages 4278–4284.
- Zhang, W. *et al.* (2017). Predicting potential drug–drug interactions by integrating chemical, biological, phenotypic and network data. *BMC bioinformatics*, **18**(1), 1–12.

Zheng, S. *et al.* (2021). PharmKG: a dedicated knowledge graph benchmark for biomedical data mining. *Briefings in bioinformatics*, **22**(4), bbaa344.

Zuo, Y. *et al.* (2022). Vitamin C is an efficient natural product for prevention of sars-cov-2 infection by targeting ACE2 in both cell and in

vivo mouse models. *bioRxiv*.

Cannot be used for transmission.